Received: 22 October 2019 | Revised: 7 January 2020 | Accepted: 8 January 2020

DOI: 10.1002/jbm.b.34563

ORIGINAL RESEARCH REPORT

Society For Biomaterials WILEY

Development of an automated micropipette coating method for drug-coated balloons

Kirby Fuglsby[1] | Jordan A. Anderson[1,2] | Daniel Engebretson[1,2] | Sujan Lamichhane[1,2]

[1]Department of Biomedical Engineering, The University of South Dakota, Sioux Falls, South Dakota

[2]Tailored Medical Devices, Inc., Sioux Falls, South Dakota

Correspondence
Sujan Lamichhane, Tailored Medical Devices, Inc. 4800 North Career Avenue, Ste 221, Sioux Falls, SD 57107.
Email: sujan.lamichhane@tailoredmedicaldevices.com

Funding information
FEDERAL AND STATE TECHNOLOGY (FAST) PARTNERSHIP PROGRAM

Abstract

Drug-coated balloons (DCBs) are a recent technology developed to treat peripheral artery disease (PAD). Along with a suitable formulation of antiproliferative drug and excipient, coating method is an important aspect of a DCB as these factors affect coating characteristics and drug delivery to the treatment site. The multiple release tailored medical devices DCB (MR-TMD-DCB), designed to achieve multiple inflations to treat complex PAD, contains paclitaxel (PAT) as the antiproliferative drug and polyethylene oxide (PEO) as the excipient. In our previous studies, the MR-TMD-DCB was coated using a manual dip coating method. In this study, an automated micropipette coating method was developed using a modified spray coating instrument to coat the MR-TMD-DCB. First, the coating formulation and strategy was optimized. A drug formulation of 16 wt% PAT and 4% wt/vol PEO, a polymer formulation of 2.5% wt/vol PEO, and a total of two drug layers produced a mostly uniform and thin coating with no defects and acceptable drug load. The balloon also had optimal drug uptake in arterial tissue in an in vitro flow model. Next, the reproducibility of the coating strategy was improved by optimizing the instrument parameters. The optimized instrument parameters (translational speed = 0.150 in/s, revolution rate = 100 rpm, flow rate = 0.6 ml/min) resulted in improved reproducibility of the drug load and similar coating properties as the DCB. This study demonstrated the ability to automate the micropipette process to obtain a balloon with optimal coating properties and drug tissue uptake.

KEYWORDS
angioplasty, dip coating method, drug-coated balloon, micropipetting method, peripheral artery disease

1 | INTRODUCTION

Drug-coated balloons (DCBs) are the proven gold standard treatment for peripheral artery disease (PAD). The antiproliferative drug, polymer excipient, and coating method are all important aspects to consider when developing DCBs. Paclitaxel is the most common antiproliferative drug used in DCBs due to its lipophilic nature and rapid uptake by the arterial wall (De Labriolle et al., 2009; Speck, Stolzenburg, Peters, & Scheller, 2015). Polymer excipients are chosen based on their ability to reduce drug loss in transit to the treatment site and improve drug transfer to the artery wall (Tesfamariam, 2016). Once the antiproliferative drug and excipient are established, it is important to choose an optimal coating method as this can affect various coating properties and drug delivery to the treatment site. In addition, the coating method is important to consider for manufacturing purposes as this can determine the manufacturability and reproducibility.

Micropipetting is a commonly used coating method for DCBs and is used to coat the Pantera Lux (Biotronik, Germany), DIOR (Eurocor, Germany), and Elutax (ab medica, Germany) DCBs, all of which are

used to treat coronary artery disease in Europe (Cortese & Bertoletti, 2012). In the micropipette method, drug and excipient solution is manually added to a rotating balloon using a micropipette to produce reproducible coating uniformity and drug load (Cortese & Bertoletti, 2012; Petersen et al., 2013). Other methods for coating balloons include dip coating and spray coating. Dip coating is a simplistic method where the balloon is manually dipped into the drug and excipient solution (Anderson, Lamichhane, Remund, Kelly, & Mani, 2016; Petersen et al., 2013). While the dip coat method is easy to carry out and produces a smooth coating, it is limited by its reproducibility in terms of coating uniformity and drug load (Petersen et al., 2013; Speck et al., 2015). The dip coat method is also generally performed manually, limiting its use in a manufacturing setting. Spray coating, in which the formulation is sprayed onto a balloon using an airbrush system, produces a highly uniform coating and reproducible drug loads. However, spray coating is complicated, produces a high amount of waste, and is limited by the viscosity of the solution as viscous solutions clog the spraying apparatus (Petersen et al., 2013; Turner, Atigh, Erwin, Christians, & Yazdani, 2018).

Recently, a multiple release tailored medical devices DCB (MR-TMD-DCB) was developed for the treatment of complex PAD with long, diffuse, and multiple lesions using a single balloon that allows multiple inflations (Anderson et al., 2019). These DCBs showed great potential in short term animal studies. However, the manufacturing reproducibility of MR-TMD-DCB is limited by its coating method. Currently, a manual dip coat method is used to coat the MR-TMD-DCB, producing nonreproducible results in terms of drug loading (Anderson et al., 2019). The formulations used to coat the MR-TMD-DCB (polyethylene oxide [PEO] and paclitaxel) are also highly viscous, limiting the use of spray coating (Petersen et al., 2013; Turner et al., 2018). The micropipette method may be an alternative method to coat the MR-TMD-DCB as it works well with viscous coating solution, and can be automated to obtain reproducible coating uniformity and drug load (Petersen et al., 2013).

Woolford et al. recently modified a stent spray coater to coat balloons using an automated micropipette method (Woolford et al., 2019). By modifying different parameters of the instrument such as revolution rate, flow rate, and translational speed, an optimal, uniform balloon coating was achieved. The resulting coating was also reproducible and demonstrated appropriate drug release kinetics in vitro (Woolford et al., 2019).

In this study, an automated micropipette method was developed to coat the MR-TMD-DCB. The coating formulation was first optimized by assessing different combinations of drug formulation, excipient formulation, and the number of drug layers for coating

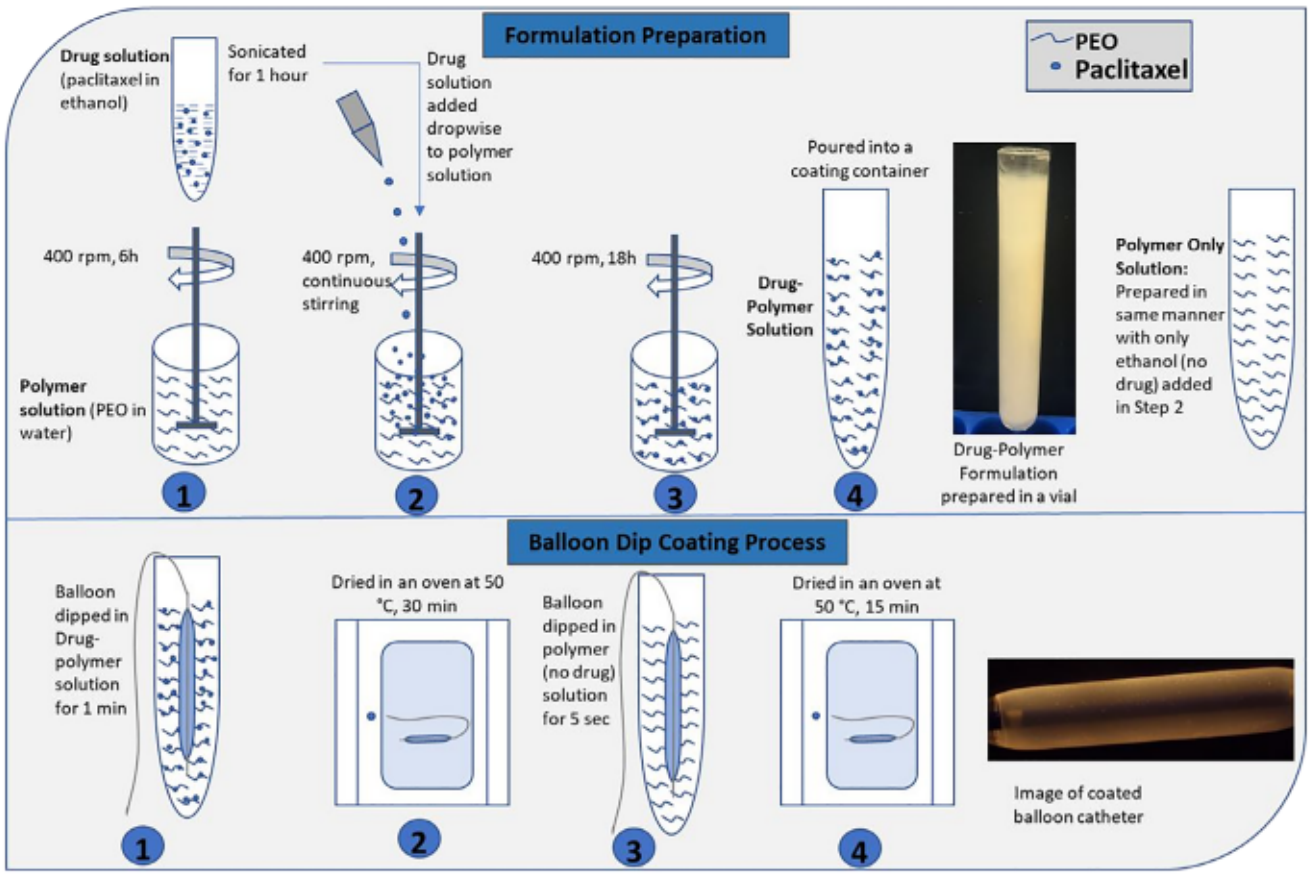

FIGURE 1 Schematic for the preparation process of coating formulation and dip coating method used for multiple-release tailored medical devices drug-coated balloons

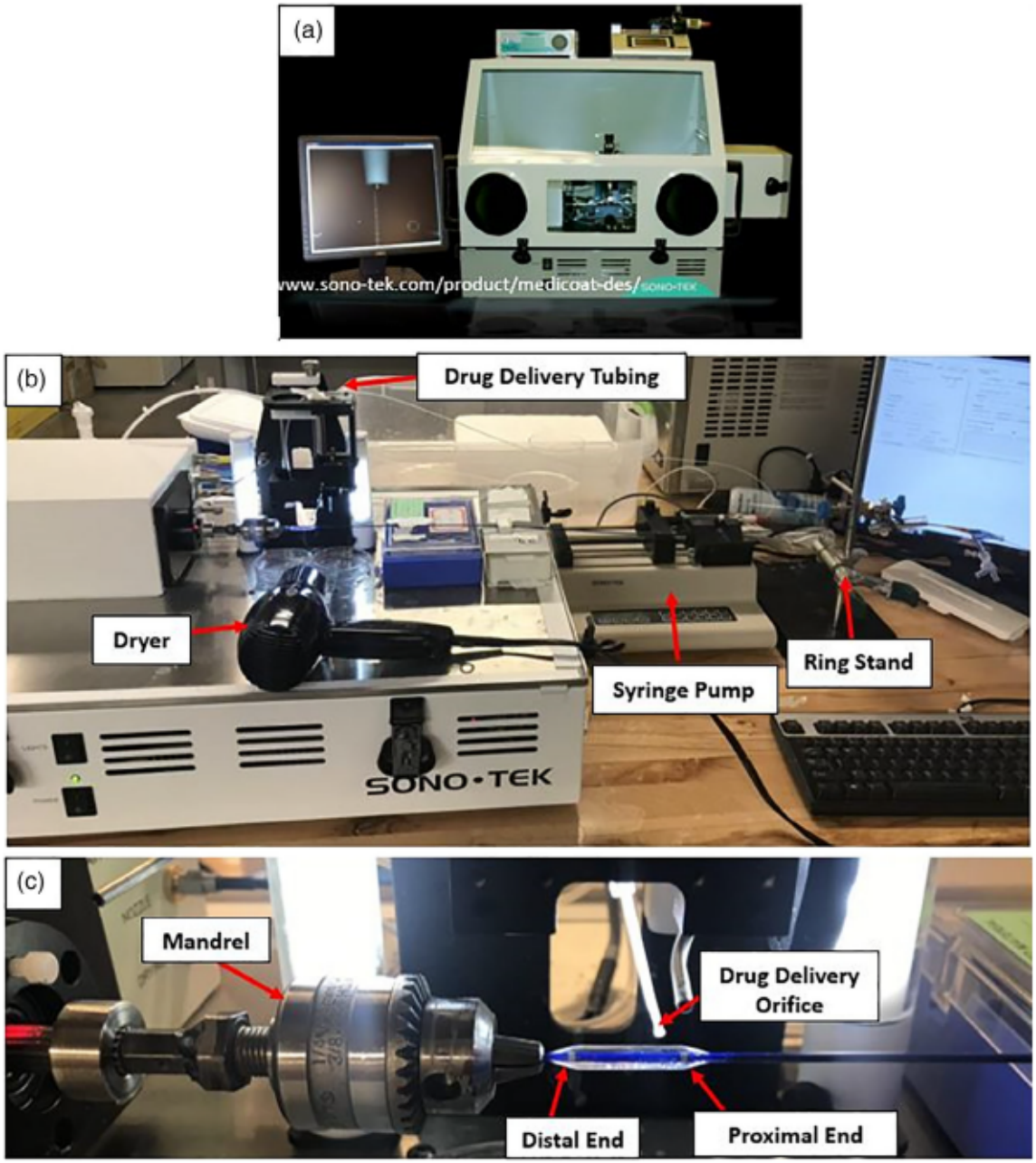

FIGURE 2 Micropipette instrument setup. (a) A Sono-Tek Medi-Coat DES ultrasonic spray coater prior to modification for micropipette coating. (b) The modified spray coater for micropipette coating application. The system consists of a syringe pump connected to drug delivery tubing. A ring stand with a tubing stabilizes the balloon. A hair dryer was used to dry the balloon. (c) The guide wire and distal end of the balloon insert into a mandrel connected to a stepper motor to rotate and move the balloon translationally. The end of the drug delivery tubing is positioned just above the balloon during coating and acts as the micropipette tip

morphology, drug load, chemical and thermal properties, and performance in an in vitro peripheral artery flow model. Next, instrument parameters including translational speed, flow rate, and revolution rate were optimized to improve the reproducibility of the balloon coating. The micropipette DCB (Mp-DCB) with optimized coating formulation and instrument parameters was then compared to the previously developed DCB developed using the dip coating method (Dp-DCB).

2 | METHODS

2.1 | Materials

PEO (average M_v 100,000), ethanol (200 proof), phosphate buffered saline (PBS), methanol, high performance liquid chromatography (HPLC) grade water, and acetonitrile were purchased from Sigma-Aldrich (St. Louis, MO). Paclitaxel (PAT)

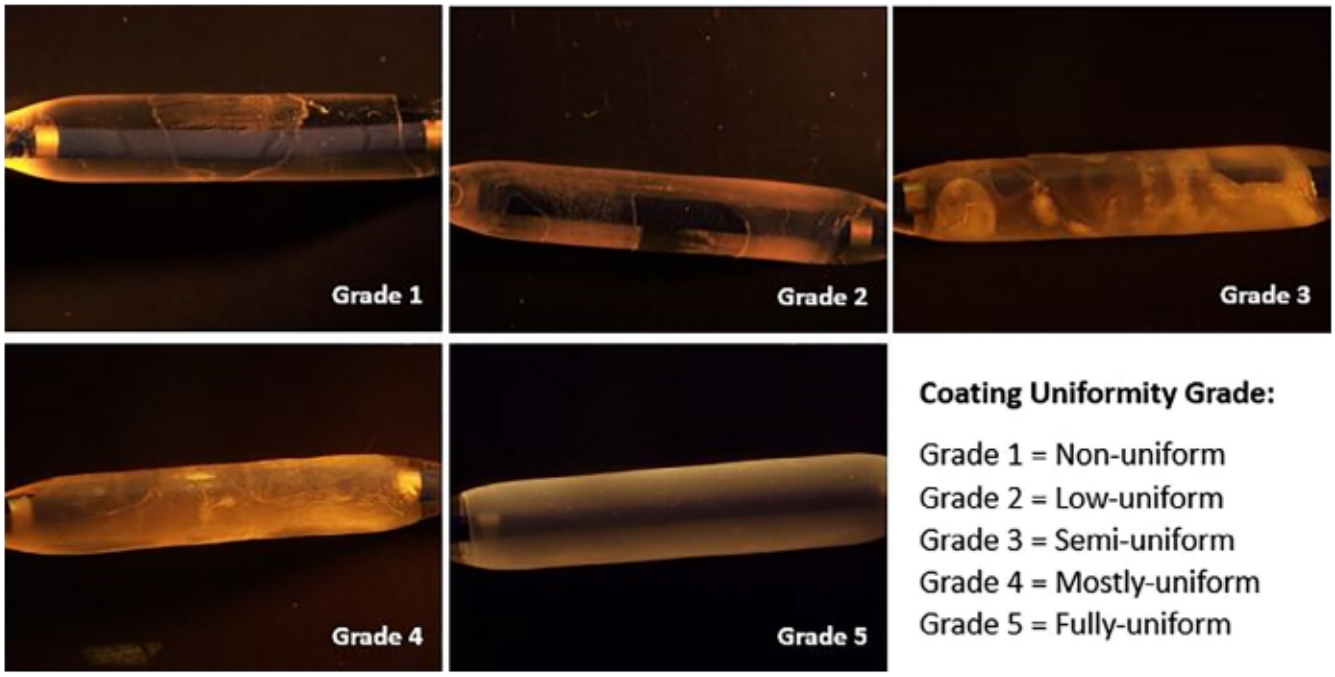

FIGURE 3 Representative images for coating uniformity grades using low magnification images from a camera attached to a light microscope

FIGURE 4 Experimental strategy for optimization of formulation and coating strategy for the micropipette method

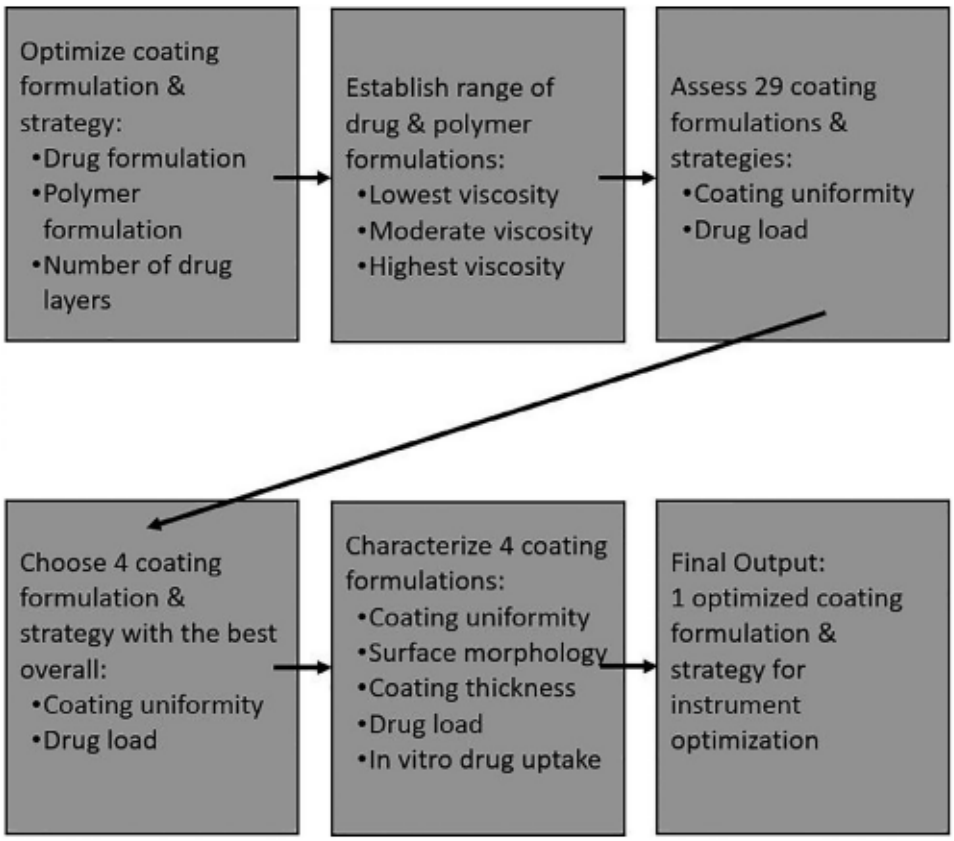

was purchased from ChemieTek (Indianapolis, IN) and the balloon inflation device was purchased from Boston Scientific (Marlborough, MA). All chemicals purchased were used as received.

2.2 | Preparation of coating formulations

PEO was sterilized prior to use by ethylene oxide. The coating formulation was prepared as previously described (Anderson et al., 2019).

TABLE 1 Optimization of formulation and coating strategy for the micropipette method. Different combinations of drug formulation, polymer formulation, and drug coating layers were assessed for the total drug amount loaded unto the balloon using HPLC and the uniformity of the coating using a grading scale. Bolded text indicates balloon was used for further characterization. For HPLC, $n = 3$ balloons were used and for coating uniformity, $n = 2$ balloons were used. Total drug amount is shown as mean ± *SD*

Balloon number	Drug formulation	Polymer formulation	Drug coating layers	Total drug amount ($\mu g/mm^2$)	Coating uniformity (scale)
1	4 wt% PAT, 1% wt/vol PEO	2.5% wt/vol PEO	1	0.41 ± 0.09	Grade 2
2	10 wt% PAT, 2.5% wt/vol PEO	2.5% wt/vol PEO	1	1.23 ± 0.26	Grade 2
3	20 wt% PAT, 5% wt/vol PEO	2.5% wt/vol PEO	1	6.57 ± 0.80	Grade 3
4	**25 wt% PAT, 6.25% wt/vol PEO**	**2.5% wt/vol PEO**	**1**	**9.95 ± 1.45**	**Grade 4**
5	26 wt% PAT, 6.5% wt/vol PEO	2.5% wt/vol PEO	1	14.48 ± 2.50	Grade 4
6	30 wt% PAT, 7.5% wt/vol PEO	2.5% wt/vol PEO	1	17.69 ± 1.87	Grade 3
7	4 wt% PAT, 1% wt/vol PEO	5% wt/vol PEO	1	0.56 ± 0.13	Grade 2
8	10 wt% PAT, 2.5% wt/vol PEO	5% wt/vol PEO	1	1.51 ± 0.61	Grade 2
9	20 wt% PAT, 5% wt/vol PEO	5% wt/vol PEO	1	5.88 ± 1.37	Grade 4
10	24 wt% PAT, 6% wt/vol PEO	5% wt/vol PEO	1	7.72 ± 0.31	Grade 4
11	**25 wt% PAT, 6.25% wt/vol PEO**	**5% wt/vol PEO**	**1**	**8.62 ± 1.68**	**Grade 4**
12	26 wt% PAT, 6.5% wt/vol PEO	5% wt/vol PEO	1	12.6 ± 1.82	Grade 4
13	30 wt% PAT, 7.5% wt/vol PEO	5% wt/vol PEO	1	17.66 ± 5.21	Grade 4
14	4 wt% PAT, 1% wt/vol PEO	2.5% wt/vol PEO	2	0.41 ± 0.11	Grade 2
15	10 wt% PAT, 2.5% wt/vol PEO	2.5% wt/vol PEO	2	2.15 ± 0.28	Grade 4
16	**16 wt% PAT, 4% wt/vol PEO**	**2.5% wt/vol PEO**	**2**	**10.08 ± 1.97**	**Grade 4**
17	16.7 wt% PAT, 4.17% wt/vol PEO	2.5% wt/vol PEO	2	11.29 ± 1.34	Grade 4
18	17 wt% PAT, 4.25% wt/vol PEO	2.5% wt/vol PEO	2	11.53 ± 1.92	Grade 4
19	18 wt% PAT, 4.5% wt/vol PEO	2.5% wt/vol PEO	2	12.93 ± 1.10	Grade 4
20	4 wt% PAT, 1% wt/vol PEO	5% wt/vol PEO	2	0.55 ± 0.10	Grade 4
21	10 wt% PAT, 2.5% wt/vol PEO	5% wt/vol PEO	2	2.53 ± 0.66	Grade 4
22	**16 wt% PAT, 4% wt/vol PEO**	**5% wt/vol PEO**	**2**	**9.01 ± 2.23**	**Grade 4**
23	16.7 wt% PAT, 4.17% wt/vol PEO	5% wt/vol PEO	2	11.51 ± 1.15	Grade 4
24	17 wt% PAT, 4.25% wt/vol PEO	5% wt/vol PEO	2	15.66 ± 4.24	Grade 4
25	18 wt% PAT, 4.5% wt/vol PEO	5% wt/vol PEO	2	11.29 ± 0.71	Grade 4
26	4 wt% PAT, 1% wt/vol PEO	2.5% wt/vol PEO	3	0.67 ± 0.22	Grade 4
27	10 wt% PAT, 2.5% wt/vol PEO	2.5% wt/vol PEO	3	3.63 ± 1.14	Grade 4
28	4 wt% PAT, 1% wt/vol PEO	5% wt/vol PEO	3	0.49 ± 0.06	Grade 4
29	10 wt% PAT, 2.5% wt/vol PEO	5% wt/vol PEO	3	4.02 ± 0.92	Grade 4
Dip coat	40 wt% PAT, 10% wt/vol PEO	5% wt/vol PEO	1	9.84 ± 1.54	Grade 5

Abbreviations: HPLC, high performance liquid chromatography; PAT, paclitaxel; PEO, polyethylene oxide.

The PAT–PEO solution was prepared by dissolving PEO (10%, wt/vol) in deionized water and allowed to stir at 400 rpm for 6 hr at room temperature. Concurrently, PAT (40 wt%) was dissolved in ethanol by sonicating for 1 hr. After 6 hr of stirring, the dissolved PAT solution was added dropwise to the PEO solution and allowed to stir at 400 rpm overnight at room temperature. The 5% wt/vol PEO solution was prepared in the same manner, but instead of adding PAT solution, the equivalent amount of ethanol was added. For micropipette coating, PAT–PEO and PEO formulations were diluted to the desired concentration using ethanol.

2.3 | Dip coating process

Dip Coated DCB (Dp-DCB) consisted of an inner layer of polymer-drug formulation and an outer layer of polymer only formulation as previously described (Anderson et al., 2019). For the dip coating process, plain balloons (EverCross PTA Balloon Catheters, 5 × 20 mm^2) were inflated to 4–6 atm and then dipped into the PAT–PEO formulation (10% wt/vol PEO, 40 wt% PAT) for 1 min and dried in a 50°C oven for 30 min. Next, the balloons were briefly submerged into the PEO (5%, wt/vol) formulation and dried in a 50°C oven for 15 min.

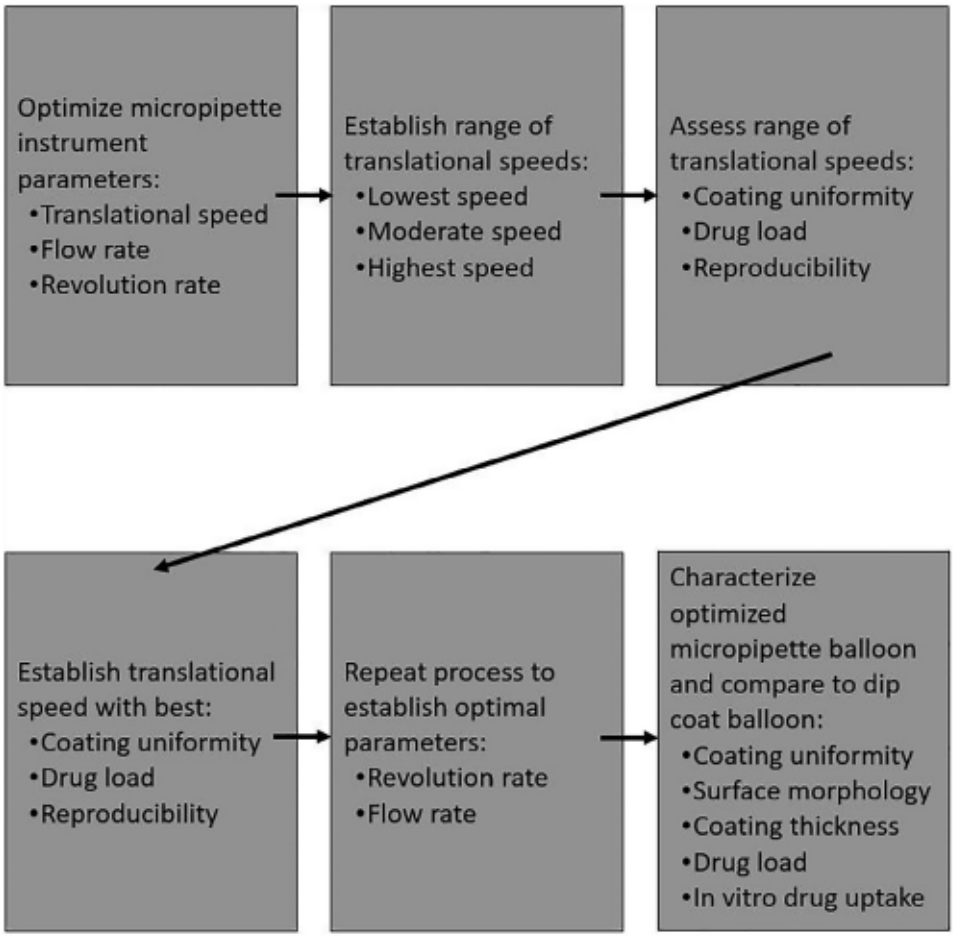

FIGURE 5 Experimental strategy for optimization of instrument parameters for Mp-DCB

Coated balloons were finally deflated and stored at room temperature until ready for use. A schematic for the dip coat process is shown in Figure 1.

2.4 | Micropipette coating process

Micropipette DCB (Mp-DCB) consisted of one to three layers of polymer-drug formulation and one layer of polymer only formulation. A Sono-Tek Medi-Coat DES 1000 ultrasonic spray coater (Sono-Tek Corporation, Milton, NY) designed to coat stents (Figure 2a) was modified for the micropipetting process to coat balloons (Figure 2b). A syringe pump attached to the spray coater pumps the coating formulation through polytetrafluoroethylene microtubing. The end of the tubing is positioned just above the balloon surface and acts as the micropipette tip to coat the balloon. Following inflation of the balloon to 4–6 atm, a guide wire is inserted through the balloon catheter and is attached at the distal end of the balloon to a mandrel. The mandrel is attached to a stepper motor that moves the balloon translationally as well as rotates the balloon while coating (Figure 2c).

Following coating, the balloon continued to rotate for 5 min while a hair dryer on low setting positioned toward the balloon blew warm air (40–50°C) to dry the coating. This process of coating and drying was repeated for subsequent PAT–PEO layers (if applicable) and for the final PEO layer for each balloon. Following coating, balloons were either used immediately for HPLC and coating uniformity analysis or deflated and stored at room temperature.

2.5 | Image characterizations

2.5.1 | Light microscope imaging

Coating uniformity was assessed using an Olympus SZX10 dissecting microscope (Olympus Corporation, Tokyo, Japan). Following coating, balloons were imaged in the inflated position and a minimum of three images at different rotational positions of each balloon were obtained. Coating uniformity was assessed using a grading scale (Figure 3).

2.5.2 | Scanning electron microscopy

Surface morphology and coating thickness were assessed using a Quanta 450 scanning electron microscope (SEM) (FEI, Hillsboro, OR). For surface morphology, the balloons were deflated then re-inflated and imaged in the inflated state. Images were obtained of the whole balloon and the distal, middle, and proximal sections at 50× magnification. Images were also obtained at 200× magnification. For coating thickness, cross sections were obtained by cutting the balloon in such a way to separate the balloon coating from the balloon surface. Cross

TABLE 2 Optimization of micropipette instrument parameters. Parameters tested included translational speed, flow rate, and revolution rate. Each parameter combination was assessed for total drug amount loaded unto the balloon via HPLC and for coating uniformity using a grading scale. Bolded text indicates the Mp-DCB that was used for further characterization and comparison to the Dp-DCB. At least $n = 3$ balloons were used for total drug amount and at least $n = 2$ balloons were used for coating uniformity. The total drug amount is shown as mean ± *SD*

Balloon	Translational speed (in/s)	Flow rate (ml/min)	Revolution rate (rpm)	Total drug amount (μg/mm²)	Coating uniformity (scale)
A	0.050	0.4	100	19.5 ± 5.6	2
B	0.100	0.4	75	13.5 ± 0.8	4
C	0.100	0.4	100	12.4 ± 1.7	4
D	0.100	0.4	150	12.6 ± 2.0	3
E	0.100	0.4	200	12.2 ± 0.7	2
F	0.125	0.4	100	12.2 ± 0.9	4
G	0.150	0.2	100	9.2 ± 2.2	4
H	0.150	0.3	100	13.7 ± 4.3	3
I	0.150	0.4	75	9.7 ± 0.9	4
J	0.150	0.4	100	11.7 ± 2.1	3
K	0.150	0.4	125	12.5 ± 0.9	4
L	0.150	0.4	150	9.3 ± 1.9	4
M	0.150	0.4	175	12.8 ± 1.2	3
N	0.150	0.4	200	10.0 ± 1.9	2
O	0.150	0.5	100	11.5 ± 2.4	4
P	**0.150**	**0.6**	**100**	**9.1 ± 0.3**	**4**
Q	0.150	0.7	100	8.4 ± 0.5	4
R	0.175	0.4	100	10.9 ± 0.2	4
S	0.200	0.4	100	11.9 ± 0.7	3

Abbreviations: Dp-DCB, dip coated DCB; HPLC, high performance liquid chromatography.

sections were obtained from the distal, middle, and proximal sections of the balloon. A minimum of three images were taken of each cross section, with five areas measured for coating thickness per image for a minimum of 45 measurements taken per each balloon.

2.6 | Thermal and chemical characterizations

To assess thermal properties of the balloon coating and crystallinity of PAT, a Q200 differential scanning calorimeter (DSC) (TA Instruments, New Castle, DE) was used. To assess chemical properties of balloon coatings, a Nicolet 6700 Fourier transform infrared (FTIR) spectrometer (Thermo Scientific, Waltham, MA) equipped with an attenuated total reflectance accessory was used. For both DSC and FTIR, PEO powder and PAT powder were used as controls. Nylon 12 balloon material was used as an additional control for DSC. PAT powder mixed with PEO powder in the same ratio as the balloon coating formulations was used as an additional control for FTIR.

2.7 | Drug quantification

For quantification of total drug loaded onto the balloon, coated balloons were placed in 30 ml of water:ethanol (50:50) solution and sonicated for 5 min or until the coating was completely dissolved from the balloon. A sample of the drug/ethanol solution was then analyzed for PAT concentration using our previously developed method using HPLC (Anderson et al., 2018).

2.8 | In vitro peripheral artery flow model analysis

2.8.1 | In vitro peripheral artery flow model

A previously developed in vitro flow model (Anderson et al., 2019) using explanted porcine carotid arteries (Smithfield Foods, Inc., Sioux Falls, SD) was used to assess drug loss, tissue uptake, and coating uniformity. The flow model was developed using a peristaltic pump that can generate a variable flow rate. A masterflex tubing of 6.4 mm diameter was used to obtain a flow of 37°C PBS solution at a rate of 200 ml/min to mimic the blood flow in peripheral arteries. A DCB insertion site was designed using a 7 Fr sheath to allow the insertion of balloon into the tubing toward the flow direction of the PBS solution. A standard inflation device designed for angioplasty balloon application was used to provide the desired inflation and deflation of the balloon. A standard guidewire was used to guide the balloon during insertion in and removal out of the in vitro model.

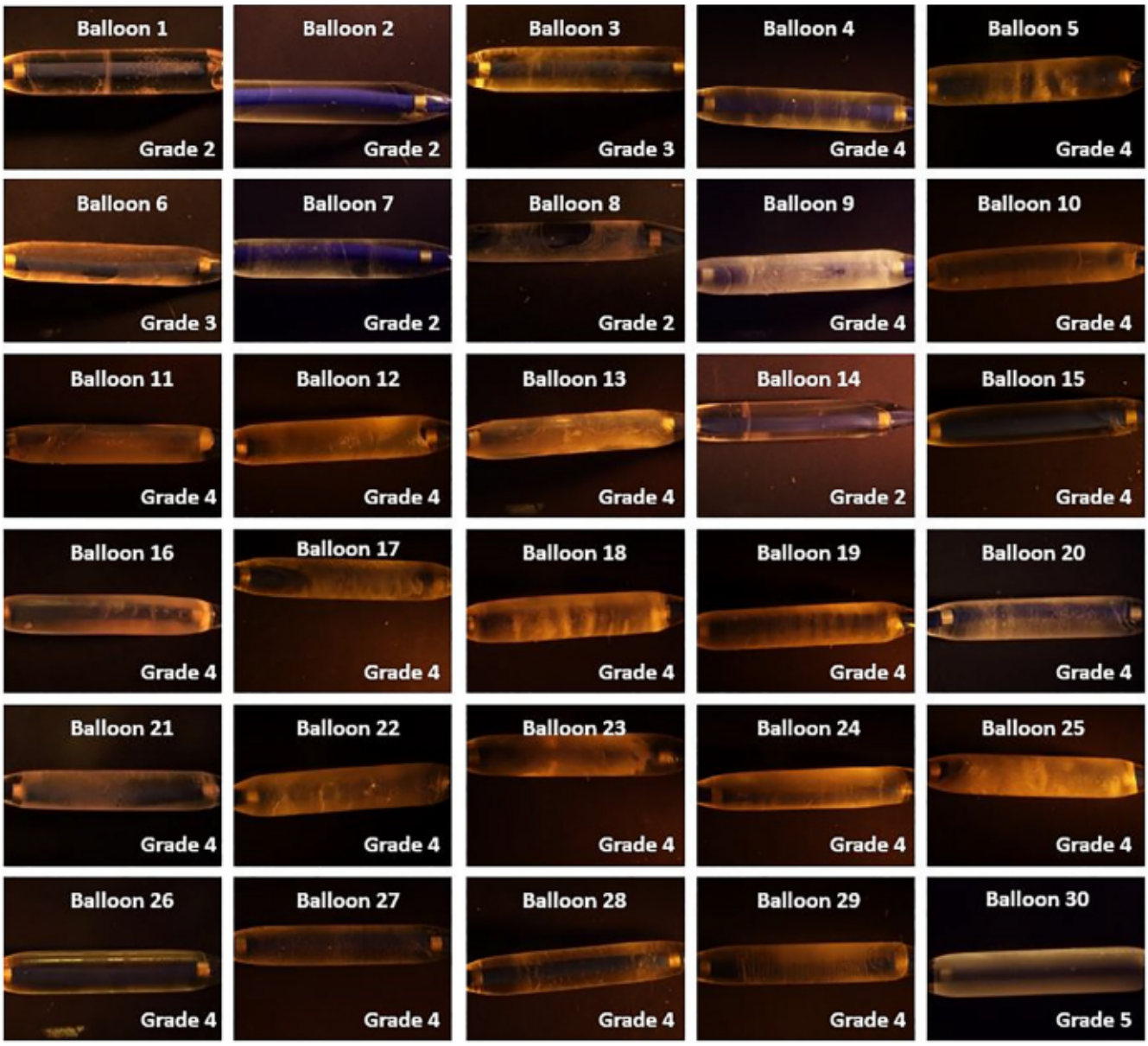

FIGURE 6 Coating uniformity of different coating formulations and strategies using the micropipette coating method. Coating formulations of varying drug formulation concentrations, polymer formulation concentrations, and number of drug layers were assigned uniformity grades ranging from nonuniform (Grade 1) to fully-uniform (Grade 5). For each coating formulation, $n = 2$ balloons were imaged. Representative images are shown

2.8.2 | Drug uptake analysis using an in vitro peripheral artery flow model

The drug uptake into the tissues was measured using a previously developed method (Anderson et al., 2018). Briefly, the deflated balloon was inserted through the sheath into the tubing using standard vascular techniques while 37°C PBS flowed through at a rate of 200 ml/min for 30 s to mimic the transit time to the first treatment site. Next, the balloon was inserted into an artery submerged in 40 ml of PBS and inflated for 30 s to assess drug uptake at the first treatment site. The balloon was then deflated and removed from the artery. Additional 37°C PBS flowed over the balloon for 30 s to mimic transit to the second treatment site. The balloon was then inserted into a second artery submerged in 40 ml of PBS and inflated for 3 min to assess drug uptake at the second treatment site. The inflation pressure of 10–12 atm was used to obtain tight fit of the balloon in the arteries during the first and second inflations. HPLC was performed on all drug containing samples (both tissues and testing fluid). A total of $n = 3$ balloons were used for each balloon type.

2.8.3 | Assessing coating uniformity using an in vitro peripheral artery flow model

To assess coating uniformity prior to each inflation (Anderson et al., 2019), the balloon was imaged using a dissecting microscope

TABLE 3 In vitro drug release of the four optimized micropipette balloon types using an in vitro peripheral artery flow model. Both the amount of drug and percentage of drug released are shown. Additional drug was lost during the inflation periods in the PBS containing solutions. For each coating formulation, $n = 3$ balloons were used. The mean ± *SD* is shown

	30 s initial loss	Drug in first artery	30 s intermediate loss	Drug in second artery	Residual drug on balloon
Balloon 4					
Drug amounts	1.9 ± 0.4 μg/mm^2	572 ± 183 ng/mg	1.4 ± 0.3 μg/mm^2	342 ± 187 ng/mg	1.2 ± 0.5 μg/mm^2
% of drug released	29 ± 6%	16 ± 4%	22 ± 5%	7 ± 2%	19 ± 8%
Balloon 11					
Drug amounts	0.9 ± 0.3 μg/mm^2	793 ± 104 ng/mg	1.8 ± 0.3 μg/mm^2	756 ± 64 μg/mm^2	1.7 ± 1.9 μg/mm^2
% of drug released	12 ± 3%	19 ± 4%	23 ± 5%	17 ± 1%	21 ± 24%
Balloon 16					
Drug amounts	1.4 ± 0.1 μg/mm^2	465 ± 107 ng/mg	1.2 ± 0.2 μg/mm^2	475 ± 105 ng/mg	3.3 ± 0.8 μg/mm^2
% of drug released	16 ± 1%	15 ± 3%	14 ± 2%	12 ± 0%	38 ± 9%
Balloon 22					
Drug amounts	1.4 ± 0.1 μg/mm^2	1,166 ± 274 ng/mg	1.0 ± 0.2 μg/mm^2	1,065 ± 332 ng/mg	1.8 ± 0.2 μg/mm^2
% of drug released	16 ± 2%	25 ± 7%	12 ± 2%	18 ± 2%	21 ± 3%

following the 30 s initial transit period and prior to inflation in the first artery. Two balloons were used for each balloon type to obtain a total of six images, with a minimum of three images obtained from each balloon. The balloon was imaged again prior to inflation in the second artery.

2.9 | Optimization of coating formulation and strategy

Figure 4 shows the study design to optimize the formulation and coating strategy of the different balloon types. A maximum of three coating layers were used to keep the coating within the desired thickness (≤75 μm) and for ease of execution. Light microscopy and HPLC were used to assess coating uniformity ($n = 2$) and HPLC ($n = 3$), respectively, on each set of drug formulation, drug coating layers, and polymer formulation balloon type combinations. Additional combinations were added until acceptable coating uniformity (Grades 4 and 5), drug load (8–10 μg/mm^2; chosen based on our previous study (Anderson et al., 2019) to deliver drug to multiple sites), and reproducibility (<25% variance) were observed in four of the balloon type combinations. The different combinations of drug formulation, polymer formulation, and drug coating layers tested are listed in Table 1. Based on the full characterization results, one balloon with the best overall results was used for optimizing the parameters on the micropipette instrument.

2.10 | Optimization of instrument parameter strategy

Figure 5 shows the study design to optimize the instrument parameters for Mp-DCB. A complete list of parameters tested can be found in Table 2. Once a combination of instrument parameters with the best coating uniformity (≥Grade 4), drug load (8–10 μg/mm^2), and reproducibility (lowest variance) was established, full characterization was performed. These results were then compared to the Dp-DCB.

2.11 | Statistical analysis

Unless otherwise specified, $n = 3$ balloons were used to carryout experiments. The data collected is represented as mean ± *SD*. A one-way analysis of variance was used to determine statistical significance at $p < .05$.

3 | RESULTS

3.1 | Formulation and coating strategy optimization

Prior to assessing the optimal coating formulations for micropipetting, the drug formulation containing 4 wt% PAT and 1% wt/vol PEO was determined to have the lowest viscosity that can still adhere to the balloon. The drug formulation containing 30 wt% PAT and 7.5% wt/vol PEO was determined to have the highest viscosity that can be pumped by the syringe pump through the drug delivery tubing. The remaining coating formulations tested were between these two concentrations. Different concentrations of PEO for the polymer only top layer were also tested in order to minimize drug loss during the initial transit period while keeping the top layer thin. The polymer formulation containing 2.5% wt/vol PEO was determined to be the lowest concentration of PEO that could still adhere to the balloon while the polymer formulation containing 5% wt/vol PEO was determined to be the highest concentration of PEO that did not cause the coating to be too thick. It was also observed that coating more than two drug layers resulted in a dramatic increase in coating thickness while not increasing the drug load onto

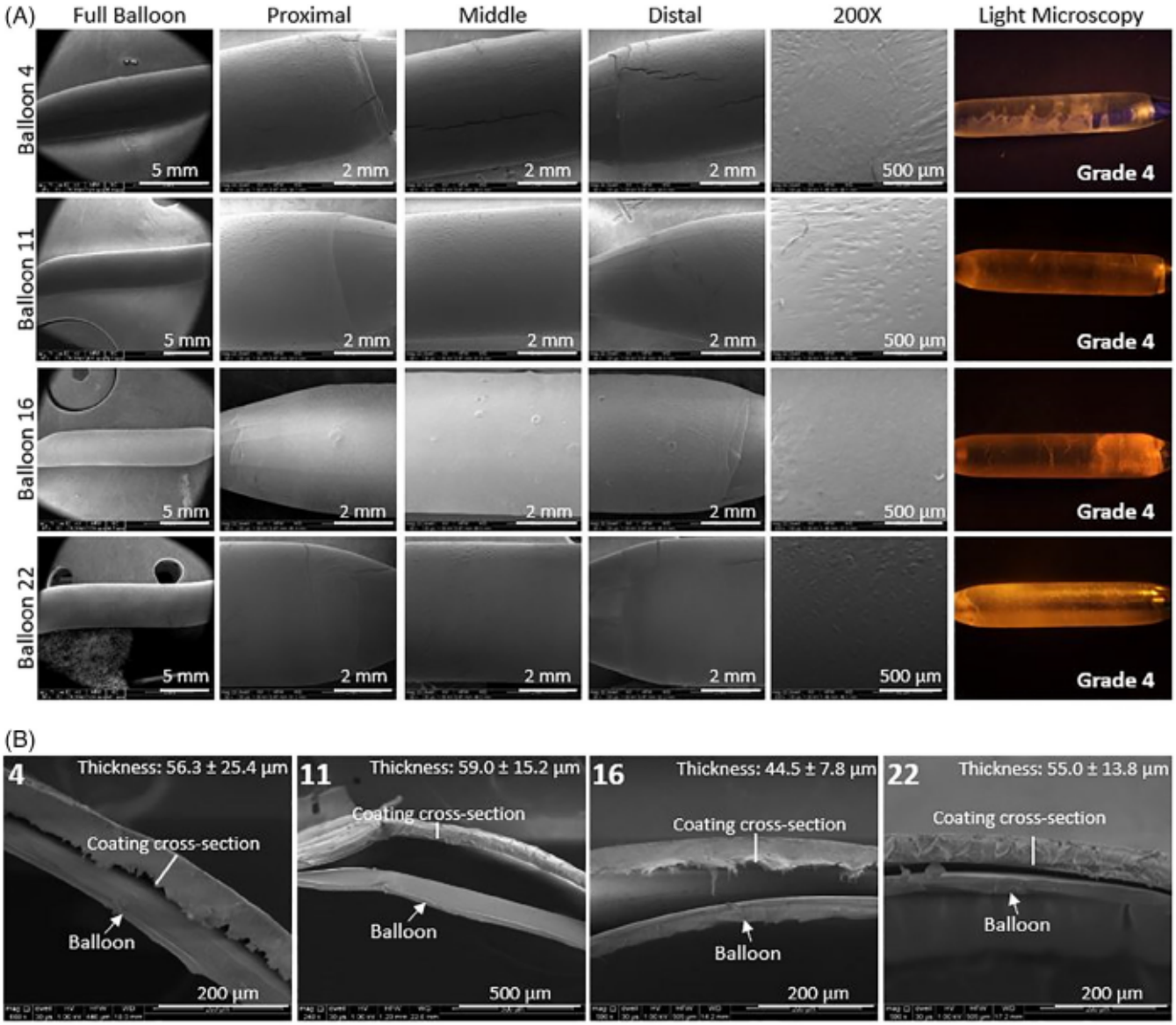

FIGURE 7 Characterization of coating morphology, uniformity, and thickness for different coating formulations. (a) Coating morphology was assessed using the following scanning electron microscope (SEM) images: full balloon, proximal section, middle section, distal section, and the surface at 200× magnification. Coating uniformity was assessed using light microscopy and assigning a grade based on uniformity. For both SEM and light microscopy, $n = 3$ balloons were imaged. Representative images are shown. (b) Cross sections were obtained from the proximal, middle, and distal sections for each different coating formulation and imaged via SEM. The thickness of the coating was measured for each cross section, with three images taken per cross section and five measurements taken per image. Representative images are shown

the balloon. Coating more than two drug layers also increased the manufacturing time. The drug formulation, polymer formulation, and number of drug layers for each coating formulation tested can be found in Table 1. Each different coating formulation was assessed for coating uniformity using light microscopy and assigning a uniformity grade based on a coating uniformity scale (Figure 3). Representative images for each balloon type are provided in Figure 6. The total amount of drug loaded onto the balloon was also assessed using HPLC (Table 1). The following four balloons from Table 1 were chosen for further characterization based on acceptable coating uniformity (Grades 4 or 5), total drug load (8–10 µg/mm^2), and reproducibility (<25% variance): Balloons 4, 11, 16, and 22.

3.2 | Characterization of four optimized formulation and coating strategy balloons

3.2.1 | Coating uniformity, morphology, and thickness

The light microscopy images all showed mostly-uniform coatings (Grade 4) for Balloons 4, 11, 16, and 22 (Figure 7a). SEM images taken of the full balloon, proximal section, middle section, distal section, and high magnification demonstrated homogenous coatings for all the Balloons 4, 11, 16, and 22 (Figure 7a). Balloons 11 and 16 demonstrated no major defects such as cracking, peeling off, or delamination.

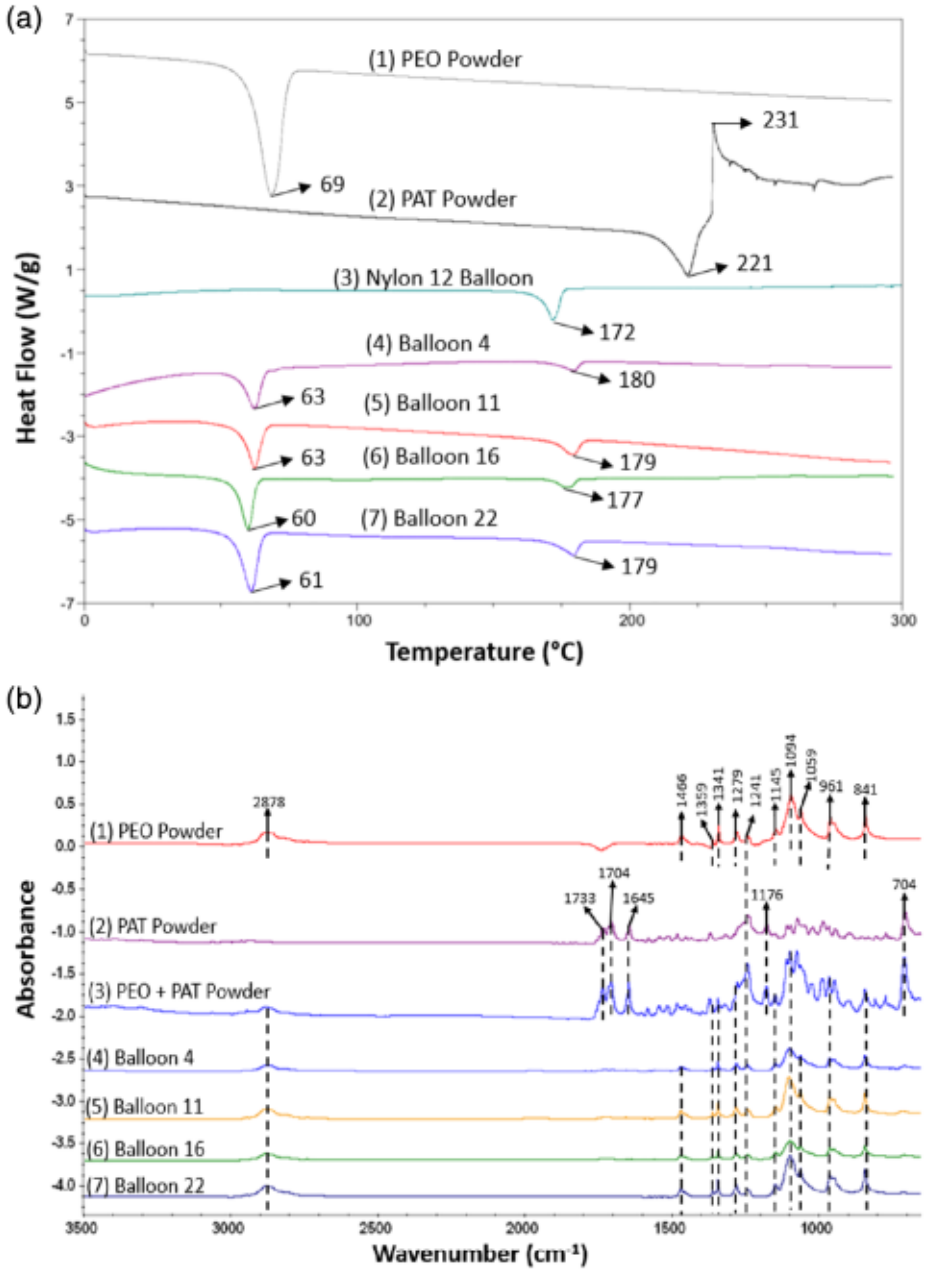

FIGURE 8 Differential scanning calorimeter (DSC) (a) and Fourier transform infrared (FTIR) (b) of the four optimized Mp-DCB

TABLE 4 In vitro drug release of the Dp-DCB and optimized Mp-DCB using a porcine explanted carotid artery model. Both the percentage and amount of drug released are shown. Additional drug was lost during the inflation periods in the PBS containing solutions. A total of $n = 3$ balloons were tested for each coating method. The mean ± *SD* is shown

	30 s initial loss	Drug in first artery	30 s intermediate loss	Drug in second artery	Residual drug on balloon
Dp-DCB					
Drug amounts	1.3 ± 0.2 μg/mm^2	569 ± 45 ng/mg	1.3 ± 0.4 μg/mm^2	411 ± 244 ng/mg	1.1 ± 0.7 μg/mm^2
% of drug released	19 ± 3%	20 ± 0%	18 ± 5%	12 ± 7%	16 ± 10%
Mp-DCB					
Drug amounts	1.5 ± 0.2 μg/mm^2	443 ± 66 ng/mg	1.3 ± 0.3 μg/mm^2	544 ± 302 ng/mg	1.0 ± 0.3 μg/mm^2
% of drug released	24 ± 4%	15 ± 1%	20 ± 4%	15 ± 7%	16 ± 5%

Abbreviations: Dp-DCB, dip coated drug coated balloon; Mp-DCB, micropipette drug coated balloon; PBS, phosphate buffered saline.

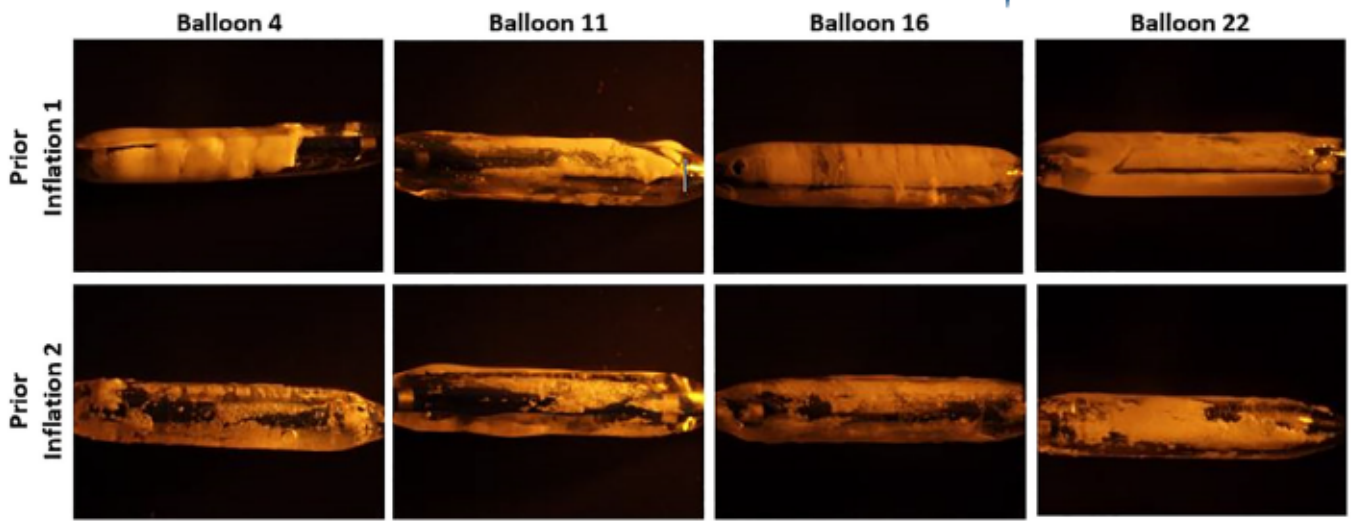

FIGURE 9 Coating uniformity of four optimized Mp-DCB balloon types prior to the first and second inflations in an in vitro peripheral artery flow model. For each coating formulation, $n = 2$ balloons were tested

Balloon 22 demonstrated minor cracking while Balloon 4 had significantly more cracking (Figure 7a).

The coating thickness for each balloon was measured using SEM images of cross sections obtained from the proximal, middle, and distal sections for each balloon. The average coating thickness for Balloons 4, 11, 16, and 22 were 56.3 ± 25.4 μm, 59.0 ± 15.2 μm, 44.5 ± 7.8 μm, and 55.0 ± 13.8 μm, respectively. Balloon 16 had a coating thickness most similar to the DCB previously reported along with the most uniform thickness amongst the four balloon coating formulations (Figure 7b) (Anderson et al., 2019).

3.2.2 | Thermal and chemical properties

DSC spectra comparing Balloons 4, 11, 16, and 22 to control PEO powder, PAT powder, and nylon 12 balloon material revealed a melting point for PEO powder at 69°C. Balloons 4, 11, 16, and 22 had similar melting points at 63, 63, 60, and 61°C, respectively. The peak observed at approximately 178°C on each of the four balloons was from the nylon 12 balloon material. The PAT powder demonstrated an endothermic peak at 221°C, indicating a crystalline nature for the PAT powder. Importantly, this peak does not exist for Balloons 4, 11, 16, or 22, indicating that PAT is in the amorphous form in the balloon coatings (Figure 8a) as previously reported (Anderson et al., 2018; Anderson et al., 2019).

For FTIR spectra, the characteristic peaks of PEO were observed in all the PEO containing samples (Anderson et al., 2016). The characteristic PAT peaks were observed only in the PAT control and PAT–PEO physical powder mixture and not in the any of the balloon samples (Anderson et al., 2016). This suggests that the PAT is molecularly dispersed in the PEO matrix of the balloon coatings (Figure 8b) as we have previously seen (Anderson et al., 2016; Anderson et al., 2018; Anderson et al., 2019).

3.2.3 | In vitro peripheral artery flow model

Prior to in vitro artery flow model studies, the total amount of drug loaded on to each balloon was quantified using HPLC ($n = 6$). Balloons 4, 11, 16, and 22 had total PAT amounts of 9.9 ± 1.4 μg/mm^2, 9.2 ± 1.5 μg/mm^2, 10.3 ± 2.1 μg/mm^2, and 9.0 ± 2.2 μg/mm^2, respectively. in vitro drug release and tissue uptake was assessed for each optimized balloon formulation using an in vitro peripheral flow model with explanted porcine carotid arteries. A complete list of amount and percentage of drug released at each step in the model is listed in Table 3. For each different formulation, $n = 3$ balloons were tested. During the initial 30 s transit period to the first treatment site (30 s initial loss), 29 ± 6%, 12 ± 3%, 14 ± 2%, and 16 ± 2% of total drug loaded was lost for Balloons 4, 11, 16, and 22, respectively. During the 30 s intermediate loss period representing the transit from the first inflation site to the second inflation site, 22 ± 5%, 23 ± 5%, 16 ± 1%, and 12 ± 2% of drug was lost for Balloons 4, 11, 16, and 22, respectively. Balloon 4 (first artery: 572 ± 183 ng/mg; second artery: 342 ± 187 ng/mg), Balloon 11 (first artery: 793 ± 104 ng/mg; second artery: 756 ± 64 ng/mg), Balloon 16 (first artery: 465 ± 107 ng/mg; second artery: 475 ± 105 ng/mg), and Balloon 22 (first artery: 1167 ± 274 ng/mg; second artery: 1066 ± 332 ng/mg) did not show significant differences in drug amounts between the first and second treatment arteries. Out of the four balloons, Balloon 16 provided the optimal results in the in vitro flow model based on its low drug loss during the transit periods while also delivering similar drug uptake in both the first and second treatment arteries.

The in vitro peripheral artery flow model was also used to assess coating uniformity before the first and second inflations. Based on observations from light microscopy images in Figure 9, the coating uniformity prior to the first inflation was mostly uniform for all four balloon types with Balloons 16 and 22 displaying a higher degree of uniformity. Prior to the second inflation, Balloon 16 had the most uniform coating compared to the other three balloon types. Therefore, Balloon 16 was

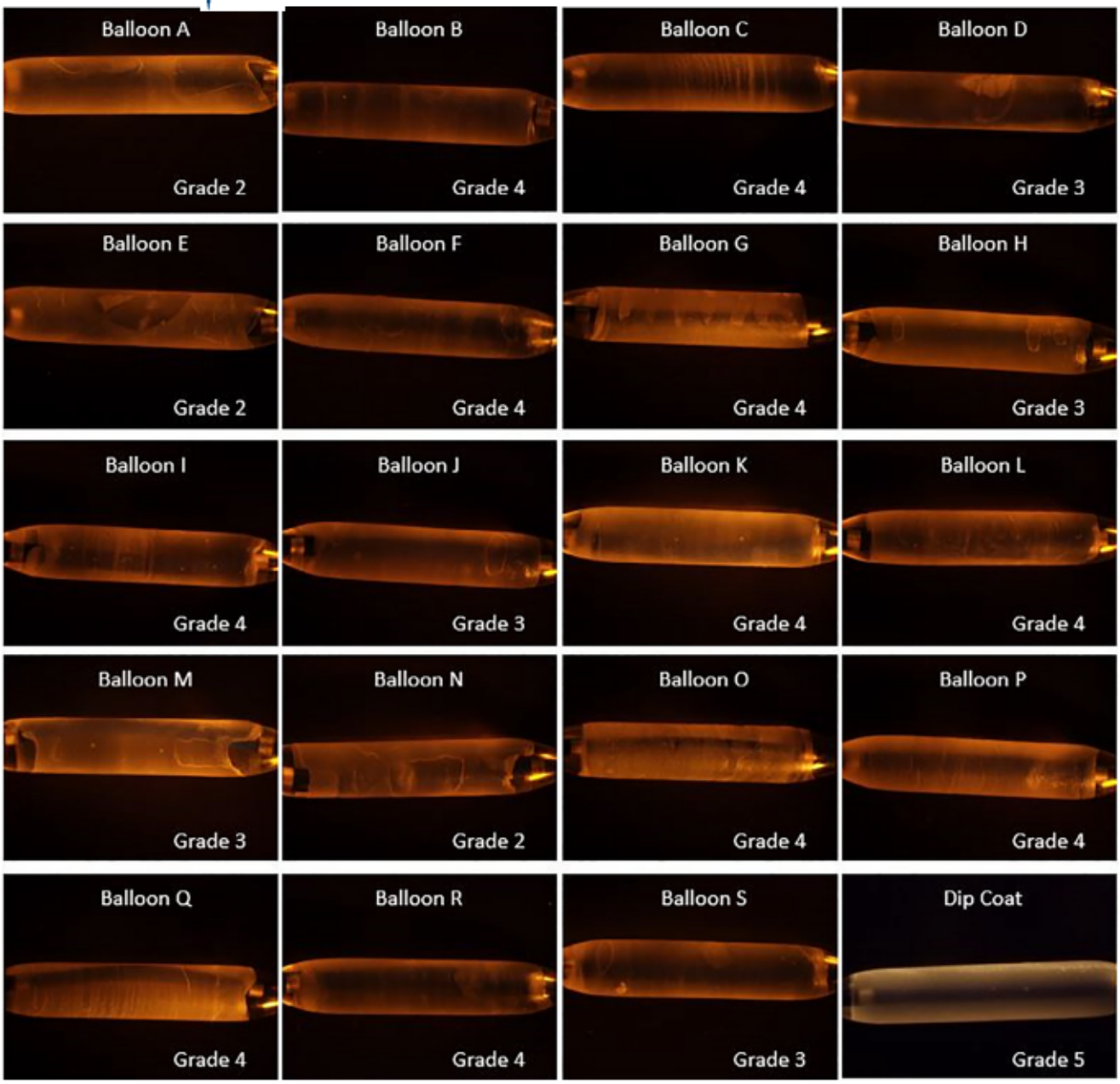

FIGURE 10 Coating uniformity of balloons developed using different instrument parameters. Each balloon was assigned a grade based on uniformity with Grade 1 being nonuniform and Grade 5 being fully uniform. At least $n = 2$ balloons were imaged for each different set of parameters. Representative images are shown. The Dp-DCB is shown for comparison

chosen as the optimal coating formulation based on the following factors: smooth and uniform coating appearance with no visible cracks, thin and uniform coating thickness, similar drug uptake in both treatment arteries, and mostly uniform coating available prior to each treatment. However, the balloon demonstrated low drug load reproducibility so further instrument parameter optimization was performed.

3.3 | Optimization of micropipette instrument parameters

Balloon 16 coating formulation and strategy were used for all instrument parameter optimizations. The following instrument parameters were optimized: translational speed, flow rate, and revolution rate. For each parameter optimization, the lowest and highest parameter values were determined based on limitations of the instrument and the ability to produce a uniform coating. Parameter values between the lowest and highest limitations were then assessed for coating uniformity, total drug load, and reproducibility. A list of parameters tested and the results for each balloon are provided in Table 2. Coating uniformity was assessed using a light microscope and the grading system in Figure 3. Representative images of the coating uniformity for each instrument parameter are shown in Figure 10. Balloon P had the set of parameters with the optimal combination of coating uniformity (≥Grade 4), acceptable drug load (8–10 μg/mm^2), and drug load reproducibility (lowest variance) (Table 2). Balloon P (optimized

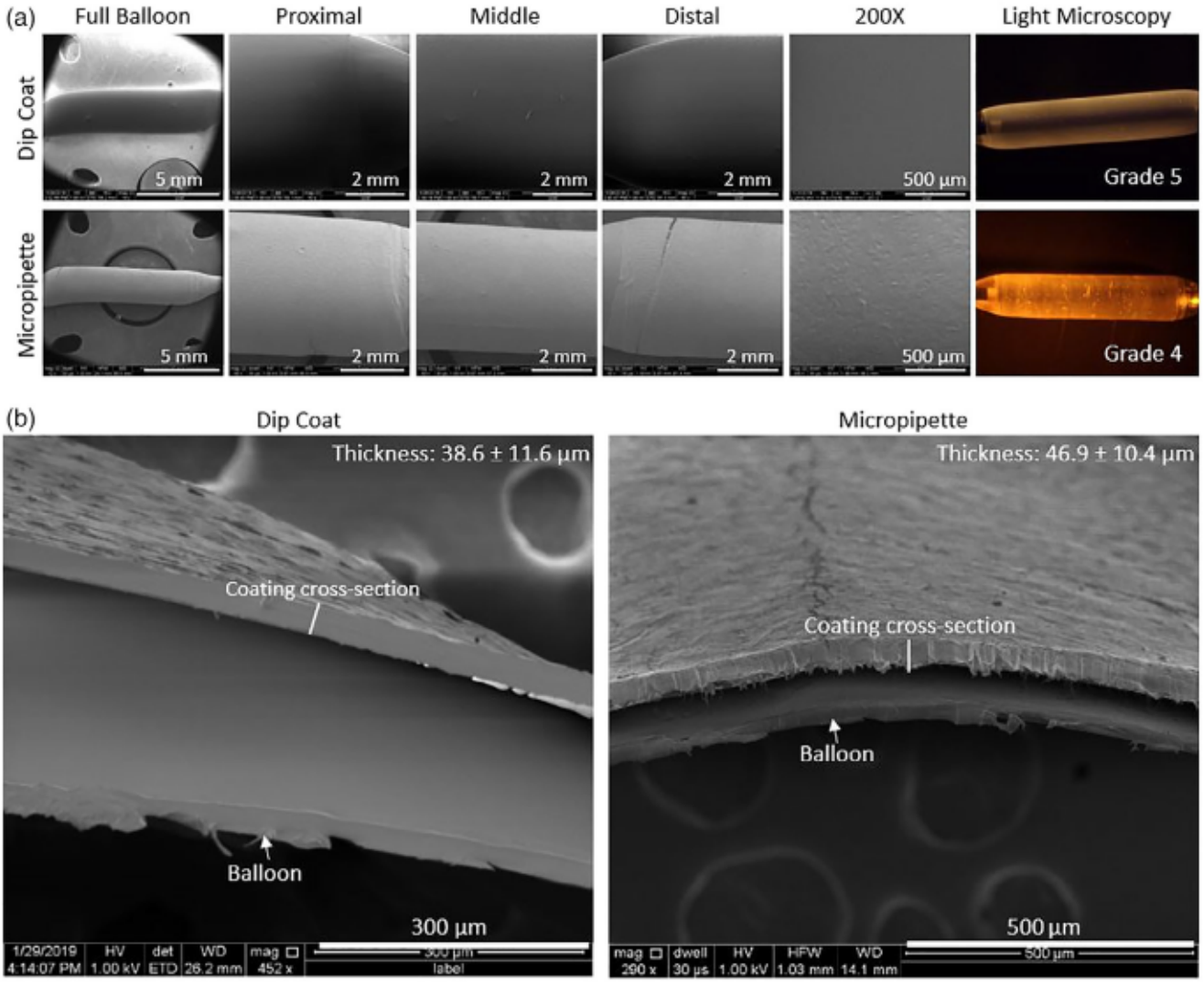

FIGURE 11 Coating uniformity, morphology, and thickness of the dip coat and the optimized micropipette balloon. (a) Scanning electron microscope (SEM) images of the full balloon, proximal section, middle section, distal section, and surface at 200× magnification and light microscopy images displaying the uniformity grade. For both SEM and light microscopy, $n = 3$ balloons were imaged. Representative images are shown. (b) Representative SEM cross-sectional images showing average coating thickness. Cross sections were obtained from the proximal, middle, and distal sections. A minimum of three images were taken for each cross section, with five measurements taken per image

micropipette balloon) was further characterized for coating uniformity, morphology, thickness, thermal and chemical properties, and in vitro peripheral artery flow model analysis. These results were compared to the Dp-DCB to assess the differences between each coating method.

3.4 | Characterization of optimized micropipette and dip coated DCBs

3.4.1 | Coating uniformity, morphology, and thickness

Coating uniformity was assessed using light microscopy images taken of the balloons developed using each of the coating methods. The optimized Mp-DCB was determined to be mostly uniform (Grade 4) while the Dp-DCB was fully uniform (Grade 5, Figure 11a), indicating that the dip coat method provides a more uniform coating along the axis length of the balloon. To assess coating morphology, SEM images of the full balloon, proximal section, middle section, distal section, and at high magnification were obtained. Both the Dp-DCB and Mp-DCB displayed smooth, homogenous coatings. No major defects were observed in the Dp-DCB whereas some minor cracking was observed in the Mp-DCB (Figure 11a).

SEM was used to measure coating thickness of proximal, middle, and distal balloon cross sections. The average coating thickness for the Dp-DCB was 38.6 ± 11.6 µm giving a variance of 30% while the Mp-DCB had an average thickness of 46.9 ± 10.4 µm giving a variance of 22% (Figure 11b). Therefore, the micropipette method provided a more uniform thickness of the coating compared to the dip coat method.

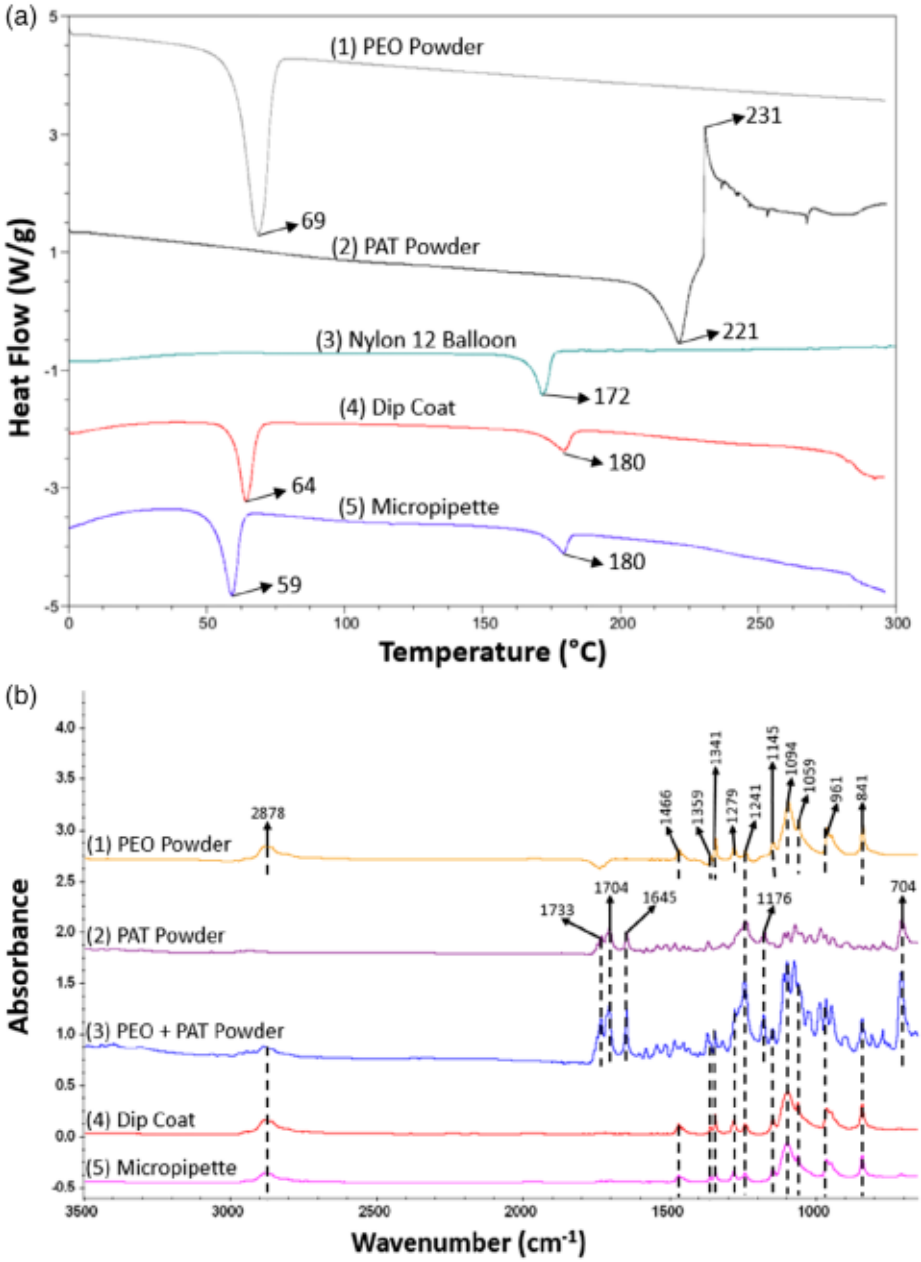

FIGURE 12 Differential scanning calorimeter (DSC) (a) and Fourier transform infrared (FTIR) (b) of the Dp-DCB and optimized Mp-DCB

3.4.2 | Thermal and chemical properties

Figure 12a shows the DSC spectra comparing the optimized Mp-DCB, the Dp-DCB, PEO powder, PAT powder, and nylon 12 balloon material. The PEO powder had a melting point of 69°C. The dip coat and micropipette balloons had similar melting points at 64 and 59°C, respectively. A melting peak for the nylon 12 balloon material was observed at 172°C and a similar peak at 180°C was present in both the dip coat and micropipette balloon. The PAT powder had an endothermic peak at 221°C, indicating its crystalline state. Neither the dip coat nor the optimized micropipette balloons contained this peak, indicating PAT remained in the amorphous nature despite the coating method used (Figure 12a).

The FTIR spectra demonstrated the characteristic peaks of PEO in the PEO powder control, PAT/PEO physical powder mixture, Dp-DCB, and optimized Mp-DCB (Anderson et al., 2016). The PAT powder and the PAT/PEO physical powder mixture demonstrated the characteristic peaks of PAT previously mentioned (Anderson et al., 2016). These peaks were absent in the dip coat and micropipette balloons, indicating that PAT remained molecularly dispersed in the PEO matrix of each balloon coating type (Figure 12b).

3.4.3 | In vitro peripheral artery flow model

Prior to in vitro studies, the total amount of drug loaded onto each balloon (n = 6) was determined to be 9.8 ± 1.4 μg/mm^2 for the Dp-

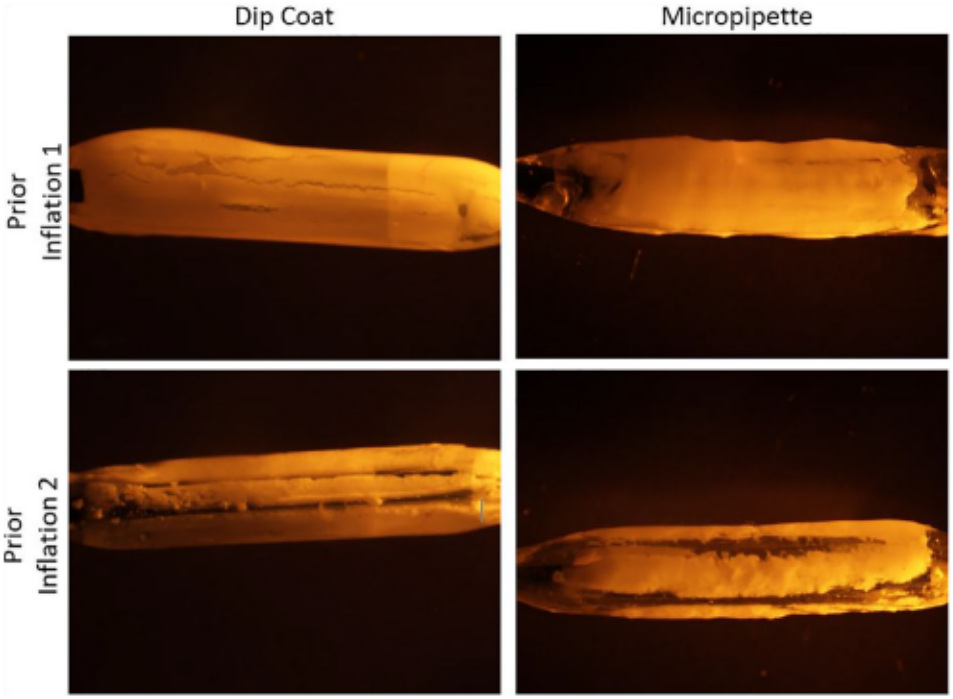

FIGURE 13 Coating uniformity of dip coat and optimized micropipette balloons prior to the first and second inflations in an in vitro model using explanted porcine carotid arteries. For each coating method, $n = 2$ balloons were imaged

TABLE 5 Advantages and disadvantages of the dip coat and micropipette coating methods for MR-TMD-DCB

	Dp-DCB	Mp-DCB
Advantages	• Ease of process • Uniform coating morphology • Coating morphology contains no major defects • Paclitaxel exists in the amorphous form • Optimal drug tissue uptake in an in vitro flow model	• Automated process • Uniform coating thickness • Improved drug load reproducibility • Paclitaxel exists in the amorphous form • Optimal drug tissue uptake in an in vitro flow model • Manufacturable in industry setting
Disadvantages	• Manual process • Increased variability in coating thickness • Decreased reproducibility of drug load	• More waste of coating formulation • Increased complexity of coating process • Possible chances of minor defects in coating morphology

Abbreviations: Dp-DCB, dip-coated DCB; Mp-DCB, micropipette DCB; MR-TMD-DCB, multiple release tailored medical devices DCB.

DCB and 9.4 ± 0.8 μg/mm^2 for the optimized Mp-DCB. Table 4 shows the results from the in vitro peripheral artery flow model comparing the Dp-DCB and Mp-DCB. During the initial 30 s transit period, 19 ± 3% of drug was lost with the Dp-DCB and 24 ± 4% of drug was lost with the Mp-DCB. During the 30 s intermediate loss period, the Dp-DCB lost 18 ± 5% of drug and the Mp-DCB lost 20 ± 4%. For the Dp-DCB, drug uptake in the first artery was 569 ± 45 ng/mg and 411 ± 244 ng/mg in the second artery. For the Mp-DCB, drug uptake in the first artery was 443 ± 66 ng/mg and 544 ± 302 ng/mg in the second artery. No significant differences in drug amount were found between the first and second arteries for either the Dp-DCB or Mp-DCB.

Figure 13 shows the images prior to the inflation in the treatment arteries in the in vitro peripheral artery flow model. The Dp-DCB and Mp-DCB were both mostly uniform prior to the first and second inflations in the treatment arteries. These results indicate that the type of coating method did not affect the drug uptake or coating uniformity through an in vitro peripheral artery flow model.

4 | DISCUSSION

The method used to coat DCBs can determine coating uniformity, morphology, thickness, drug load, drug crystallinity, and drug release, all of which are important aspects to consider when developing DCBs (Tesfamariam, 2016; Xiong et al., 2016). The coating should be uniform to deliver drug evenly to the artery wall (Seidlitz et al., 2013). Additionally, the coating should be thin, smooth, and contain minimal defects to minimize drug loss and particulate formation (Kaule et al., 2015; Seidlitz et al., 2013). The drug load should also be sufficient to deliver a therapeutic amount of drug to the treatment site (Tesfamariam, 2016). The crystallinity of PAT is also important to consider as crystalline PAT may form embolism causing particulates, an issue with current FDA approved DCBs (Kolodgie et al., 2016; Krishnan et al., 2017; Torii et al., 2019). Conversely, amorphous PAT reduces the risk of particulate formation and improves drug solubility in the tissue (Krishnan et al., 2017). The concentration of excipient and drug in the coating formulation, and the number of coating layers

applied onto the balloons can be properly tuned to reduce drug loss during transit periods and maximize the amount of drug delivered to the treatment site (Anderson et al., 2019; Tesfamariam, 2016; Xiong et al., 2016).

In this study, an automated micropipette method using a modified stent spray coater was developed and optimized for the coating of the MR-TMD-DCB. Micropipetting was chosen as the coating method based on its ability to be automated, produce a uniform and reproducible coating, and its ability to accommodate viscous drug formulations (Petersen et al., 2013). The formulation and coating strategy were first optimized by assessing the drug amount loaded onto the balloon and coating uniformity of different combinations of drug formulation, polymer formulation, and the number of drug layers coated onto balloons. Four balloons with the best combination of drug load and uniform coatings where chosen for further characterization: Balloons 4, 11, 16, and 22.

When optimizing the Mp-DCB coating, two different concentrations of polymer formulation (2.5 and 5% wt/vol PEO) were assessed. The purpose of the PEO layer in the balloon coating is to reduce the amount of drug loss in transit to the treatment site in order to deliver an optimal, therapeutic amount of PAT to the artery tissue (Anderson et al., 2019). It is also important for the PEO layer to not add too much thickness to the balloon, as this can impose difficulties in folding the balloon, increase the cross-sectional profile of the balloon, and thus complicate the passage of the balloon through the sheath (Kaule et al., 2015). When characterizing Balloons 4, 11, 16, and 22, formulations containing 2.5% PEO as the top layer was determined to be the optimal concentration of PEO to minimize drug loss in the in vitro flow model while keeping the coating thin. A drug load of 8–10 μg/mm^2 PAT was used as a desirable range so as to achieve the required tissue drug uptake in multiple treatment sites. Moreover, the MR-TMD-DCB is designed for the treatment of multiple lesions with a single balloon. If a patient was treated for two lesions with the FDA approved IN.PACT DCB, two DCBs would be used, exposing the patient to 7 μg/mm^2 of PAT as a single IN.PACT DCB contains 3.5 μg/mm^2 PAT (Peterson, Hasenbank, Silvestro, & Raina, 2017). A study by Kelsch et al. (2011) also demonstrated a balloon coated with 9 μg/mm^2 PAT was tolerated well in porcine model with no adverse events.

Of the four balloons, Balloon 16 demonstrated optimal drug load, coating uniformity and morphology, chemical, and thermal properties, and equivalent drug delivery into two separate arteries in an in vitro peripheral artery flow model. Different instrument parameters were then optimized to reduce drug load variance. The following combination of instrument parameters was determined to have optimal drug load, coating uniformity, and reproducibility: 0.150 in/s translational speed, 0.6 ml/min flow rate, and 100 rpm revolution rate. This optimized Mp-DCB was then compared to the Dp-DCB. The summary of comparison between the optimized Mp-DCB and Dp-DCB is provided in Table 5. In general, the micropipette balloon had similar properties to the DCB with better uniformity of coating thickness, and an improved drug loading reproducibility. In contrast, the dip coat method had better overall uniformity in coating morphology compared to the micropipette balloon. Importantly, PAT remained amorphous and molecularly dispersed in the PEO matrix in the Mp-DCB (Anderson et al., 2018; Anderson et al., 2019).

While the optimized Mp-DCB demonstrated similar characteristics compared to the Dp-DCB, further optimization is needed. This includes improving the coating uniformity along the axis length of the balloon to consistently achieve a fully uniform coating with no defects such as cracking. Moreover, further optimization of the micropipette may improve the reproducibility to a greater extent. The micropipette process may be improved by encasing the system in an inert atmosphere, which may help to spread the coating more evenly around the balloon. Moreover, in the current micropipette apparatus, a hair dryer was used to dry the balloon coating. Airflow was therefore based on hair dryer settings and the temperature was controlled based on the distance the dryer was placed from the balloon. The addition of a built-in heating system may improve the micropipette system as it would be easier to control the temperature and airflow to dry the coating. In the future, it may also be beneficial to develop an automated dip coat method and compare the coating to the automated micropipette method.

5 | CONCLUSIONS

This study demonstrated the feasibility to develop an automated micropipette method for coating a DCB designed to treat multiple lesions. The coating formulation and strategy along with instrument parameters were optimized to produce a balloon with a mostly uniform, thin coating with minimal defects and a desirable reproducible drug load. Moreover, the resulting micropipette coating demonstrated optimal drug uptake in arterial tissue in an in vitro flow model and had characteristics similar to a balloon coated using the dip coat method.

REFERENCES

Anderson, J. A., Lamichhane, S., Fuglsby, K., Remund, T., Pohlson, K., Evans, R., … Kelly, P. (2019). Development of drug-coated balloon for the treatment of multiple peripheral artery segments. *Journal of Vascular Surgery*. https://doi.org/10.1016/j.jvs.2019.04.494.

Anderson, J. A., Lamichhane, S., Remund, T., Kelly, P., & Mani, G. (2016). Preparation, characterization, in vitro drug release, and cellular interactions of tailored paclitaxel releasing polyethylene oxide films for drug-coated balloons. *Acta Biomaterialia*, *29*, 333–351.

Anderson, J. A., Lamichhane, S., Vierhout, T., Sherman, A., Engebretson, D., Pohlson, K., … Kelly, P. (2018). In vitro particulate and in vivo drug retention study of a novel polyethylene oxide formulation for drug-coated balloons. *Journal of Vascular Surgery*, *67*(5), 1537.e7–1545.e7.

Cortese, B., & Bertoletti, A. (2012). Paclitaxel coated balloons for coronary artery interventions: A comprehensive review of preclinical and clinical data. *International Journal of Cardiology*, *161*(1), 4–12.

De Labriolle, A., Pakala, R., Bonello, L., Lemesle, G., Scheinowitz, M., & Waksman, R. (2009). Paclitaxel-eluting balloon: From bench to bed. *Catheterization and Cardiovascular Interventions*, *73*(5), 643–652.

Kaule, S., Minrath, I., Stein, F., Kragl, U., Schmidt, W., Schmitz, K. P., … Petersen, S. (2015). Correlating coating characteristics with the performance of drug-coated balloons—A comparative in vitro investigation

of own established hydrogel- and ionic liquid-based coating matrices. *PLoS One*, *10*(3), e0116080.

Kelsch, B., Scheller, B., Biedermann, M., Clever, Y. P., Schaffner, S., Mahnkopf, D., … Cremers, B. (2011). Dose response to paclitaxel-coated balloon catheters in the porcine coronary overstretch and stent implantation model. *Investigative Radiology*, *46*(4), 255–263.

Kolodgie, F. D., Pacheco, E., Yahagi, K., Mori, H., Ladich, E., & Virmani, R. (2016). Comparison of particulate embolization after femoral artery treatment with IN.PACT admiral versus Lutonix 035 paclitaxel-coated balloons in healthy swine. *Journal of Vascular and Interventional Radiology*, *27*(11), 1676 e2–1685 e2.

Krishnan, P., Faries, P., Niazi, K., Jain, A., Sachar, R., Bachinsky, W.B., … Lyden, S.P. (2017). Stellarex drug-coated balloon for treatment of femoropopliteal disease: Twelve-month outcomes from the randomized ILLUMENATE pivotal and pharmacokinetic studies. *Circulation*, *136*(12), 1102–1113.

Petersen, S., Kaule, S., Stein, F., Minrath, I., Schmitz, K. P., Kragl, U., & Sternberg, K. (2013). Novel paclitaxel-coated angioplasty balloon catheter based on cetylpyridinium salicylate: Preparation, characterization and simulated use in an in vitro vessel model. *Materials Science & Engineering. C, Materials for Biological Applications*, *33*(7), 4244–4250.

Peterson, S., Hasenbank, M., Silvestro, C., & Raina, S. (2017). IN.PACT admiral drug-coated balloon: Durable, consistent and safe treatment for femoropopliteal peripheral artery disease. *Advanced Drug Delivery Reviews*, *112*, 69–77.

Seidlitz, A., Kotzan, N., Nagel, S., Reske, T., Grabow, N., Harder, C., … Weitschies, W. (2013). In vitro determination of drug transfer from drug-coated balloons. *PLoS One*, *8*(12), e83992.

Speck, U., Stolzenburg, N., Peters, D., & Scheller, B. (2015). How does a drug-coated balloon work? Overview about coating technologies and their impact. *The Journal of Cardiovascular Surgery*, *57*(1), 3-11.

Tesfamariam, B. (2016). Local arterial wall drug delivery using balloon catheter system. *Journal of Controlled Release*, *238*, 149–156.

Torii, S., Jinnouchi, H., Sakamoto, A., Romero, M. E., Kolodgie, F. D., Virmani, R., & Finn, A. V. (2019). Comparison of biologic effect and particulate embolization after femoral artery treatment with three drug-coated balloons in healthy swine model. *Journal of Vascular and Interventional Radiology*, *30*(1), 103–109.

Turner, E. A., Atigh, M. K., Erwin, M. M., Christians, U., & Yazdani, S. K. (2018). Coating and pharmacokinetic evaluation of air spray coated drug coated balloons. *Cardiovascular Engineering and Technology*, *9*(2), 240–250.

Woolford, S. E., Tran, M., NguyenPho, A., McDermott, M. K., Oktem, B., & Wickramasekara, S. (2019). Optimization of balloon coating process for paclitaxel coated balloons via micro-pipetting method. *International Journal of Pharmaceutics*, *554*, 312–321.

Xiong, G. M., Ang, H., Lin, J., Lui, Y. S., Phua, J. L., Chan, J. N., … Huang, Y. (2016). Materials technology in drug eluting balloons: Current and future perspectives. *Journal of Controlled Release*, *239*, 92–106.

How to cite this article: Fuglsby K, Anderson JA, Engebretson D, Lamichhane S. Development of an automated micropipette coating method for drug-coated balloons. *J Biomed Mater Res.* 2020;108B:2258–2275. https://doi.org/10.1002/jbm.b.34563